IEEE/CSC & ESAS EUROPEAN SUPERCONDUCTIVITY NEWS FORUM (ESNF), No. 18, October 2011
Submitted to ESNF July 28, 2011; accepted October 06, 2011. Reference ST274, Category 4
Published in *Journal of Low Temperature Physics* **167**, Numbers 3-4, 188-194 (2012)

A Distributed TES Model for Designing Low Noise Bolometers Approaching SAFARI Instrument Requirements

P. Khosropanah[1*] , R.A. Hijmering[1] , M. Ridder[1] , M.A. Lindeman[1], L. Gottardi[1] , M. Bruijn[1] , J. van der Kuur[1] , P.A.J. de Korte[1] , J.R. Gao[1,2] , H. Hoevers[1]

1 SRON Netherlands Institute for Space Research, Sorbonnelaan 2, 3584 CA Utrecht, The Netherlands
2 Kavli Institute of NanoScience, Delft University of Technology, Lorentzweg 1, 2628 CJ Delft, The Netherlands

Transition edge sensors (TES) are the chosen detector technology for the SAFARI imaging spectrometer on the SPICA telescope. The TES are required to have an NEP of 2-3×10^{-19} W/√Hz to take full advantage of the cooled mirror. SRON has developed TiAu TES bolometers for the short wavelength band (30-60 μm). The TES are on SiN membranes, in which long and narrow legs act as thermal links between the TES and the bath. We present a distributed model that accounts for the heat conductance and the heat capacity in the long legs that provides a guideline for designing low noise detectors. We report our latest results that include a measured dark NEP of 4.2×10^{-19} W/√Hz and a saturation power of about 10 fW.
PACS numbers: 85.25.Pb, 95.85.Gn

1. INTRODUCTION

SPICA[1] is a Japanese-led mission to fly a 3.5 m diameter IR telescope with a cryogenically cooled mirror (~5K). Cooling the optics reduces the background radiation caused by the ambient temperature of the FIR space telescopes that limits the sensitivity. The loading is then dominated by astrophysical background sources. The SAFARI[2] instrument is an imaging Fourier Transform Spectrometer (FTS) on SPICA with three bands covering the wavelength ranges: 35-60 μm, 60-110 μm, and 110-210 μm. The background radiation in these bands is estimated by emission from the Zodiacal light at a level of 0.3-1 fw.[2] This gives a photon noise equivalent power (NEP) at the detectors of 1-3×10^{-18} W/√Hz. Therefore, we require detectors with electrical NEPs at least 3 times lower than the photon noise limit, i.e. ≤ 3×10^{-19} W/√Hz. This is about 2 orders of magnitude higher

sensitivity than what is required for detectors on a ground based telescope and impose a great challenge on the detector technology.

Transition edge sensor (TES) is the chosen detector for the SAFARI instrument. In collaboration with a European institutes, SRON is developing low thermal conductance TES bolometers that are based on Ti/Au bilayer as sensitive element on suspended silicon nitride (SiN) membranes.

The measured dark NEPs in our original devices were typically a factor of 2-3 higher than what were expected from the measured thermal conductance. Here we argue that part of the excess noise is due to the thermal fluctuation in the supporting legs and present a distributed leg model that provides a guideline for designing low noise devices. We then support the model by our latest measurement results.

2. DISTRIBUTED MODEL

The simplest TES model consists of a heat capacity C_{TES} connected to the bath with a heat conductance G_{TES}. The electrical-thermal equations that follow from this model were introduced by M.A. Lindeman.[3] In the low-G devices as the legs are very long the mass and the heat capacity of the legs are considerable compared to that of the TES and the SiN island. The temperature along the legs also varies between the T_C and the T_{bath}. A way to model this would be to consider the legs as a series of bodies with certain heat capacities at different temperature that are connected with series of G's as shown in Fig. 1. Writing the small signal heat balance equations similar to the simple model leads us the following impedance matrix that can be used to calculate the noise, responsivity and the complex impedance of the TES.

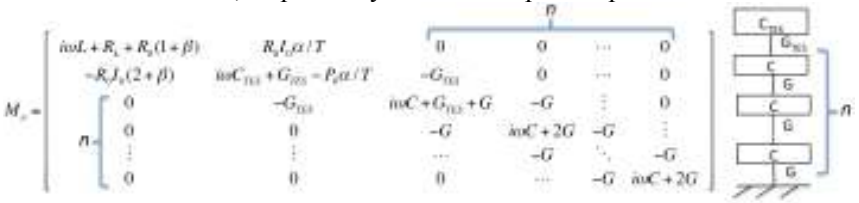

Fig. 1. Distributed leg model and the resulting impedance matrix from the small signal electrical-thermal equations.

Here R_L is the loading resistance and L is the inductance in the bias circuit. T_0 is the temperature of the device, R_0 is the resistance of the TES, I_0 is the *dc* current that runs through the device and P_0 is the corresponding *dc* power. α is the resistance dependence of the temperature at constant bias current and β is the resistance dependence of the current at constant temperature:

A Distributed TES Model for Designing Low Noise Bolometers

$$\alpha = \frac{T_0}{R_0}\frac{\partial R}{\partial T}\bigg|_{I_0}, \quad \beta = \frac{I_0}{R_0}\frac{\partial R}{\partial I}\bigg|_{T_0}.$$

The total noise current consists of the phonon noise I_{PH}, the Johnson noise I_{JO} and the noise from the loading resistor I_L.

$$I_{TOTAL}(\omega) = \sqrt{I_{PH}^2(\omega) + I_{JO}^2(\omega) + I_L^2(\omega)},$$

where I_{JO} and I_L are:

$$I_{JO}(\omega) = \sqrt{4k_B T_0 R_0 (1+2\beta)} \cdot (M_n^{-1}(1,1) - I_0 M_n^{-1}(1,2))$$

$$I_L(\omega) = \sqrt{4k_B T_{bath} R_L} \cdot M_n^{-1}(1,1).$$

In order to calculate the phonon noise we need to know the thermal fluctuation in each of the bodies in the model and the responsivity associated with them. The responsivity of the n^{th} body is defined as $SI_n = dP_n/dI$ with P_n being the power applied to that body and I is the TES current. The responsivity and the phonon noise contribution of each of the bodies are as follows:

$$SI_0(\omega) = M_n^{-1}(1,2) \qquad I_{PH0}(\omega) = \sqrt{4\gamma_0 k_B T_0^2 G_{TES}} \cdot (SI_0(\omega) - SI_1(\omega))$$

$$SI_1(\omega) = M_n^{-1}(1,3) \qquad I_{PH1}(\omega) = \sqrt{4\gamma_1 k_B T_1^2 G} \cdot (SI_1(\omega) - SI_2(\omega))$$

$$\vdots \qquad\qquad \vdots$$

$$SI_n(\omega) = M_n^{-1}(1,n+2) \qquad I_{PHn}(\omega) = \sqrt{4\gamma_n k_B T_n^2 G} \cdot SI_n(\omega)$$

Here k_B is the Boltzmann's constant and γ_n is a number between 0.5-1 that depends on the heat transport mechanism and can be estimated as $\gamma_n = ((T_n/T_{n+1})^4+1)/2$ for each section.[4] The total phonon noise is:

$$I_{PH}(\omega) = \sqrt{I_{PH0}^2(\omega) + I_{PH1}^2(\omega) + \cdots + I_{PHn}^2(\omega)}.$$

The impedance of the device Z_{TES} can also be calculated using the matrix:

$$Z_{TES}(\omega) = M_n^{-1}(1,1) - i\omega L - R_L.$$

By setting n equal to 0, all equations above are reduced to that of the simple bolometer model. In that case M_0 will be a 2×2 matrix and there is only one responsivity (SI_0) and only one term for the phonon noise ($I_{PH}=I_{PH0}$).[5]

Fig. 2 shows the measured and modeled impedance and the noise spectra using the simple TES model (n=0) and the distributed leg model (n=10). The bias point is at 30% low in the transition. The details of this device are reported elsewhere.[6] Note that in this calculation all device parameters are identical in both models. The bias point and the total G are known from the IV curves. α, β and C_{TES} are extracted from impedance

curves. The only difference is that for the distributed leg model we estimate the C_{LEG} by comparing the geometry of the legs and the island, distribute that into 10 bodies and insert it between the TES and the bath.

As we see the measured noise is about a factor of two higher than the calculated noise at low frequencies. Besides, there is a bump in the measured noise spectra that cannot be explained by the simple model and there is a clear difference between the measured and modeled impedance curves at low frequencies. Although the distributed leg model cannot explain all the excess noise, it does predict the shape of the noise spectra and is in better agreement with the measured impedance.

Over all our modeling effort indicates that the major part of our excess noise is due to the thermal fluctuations in the long supporting legs.

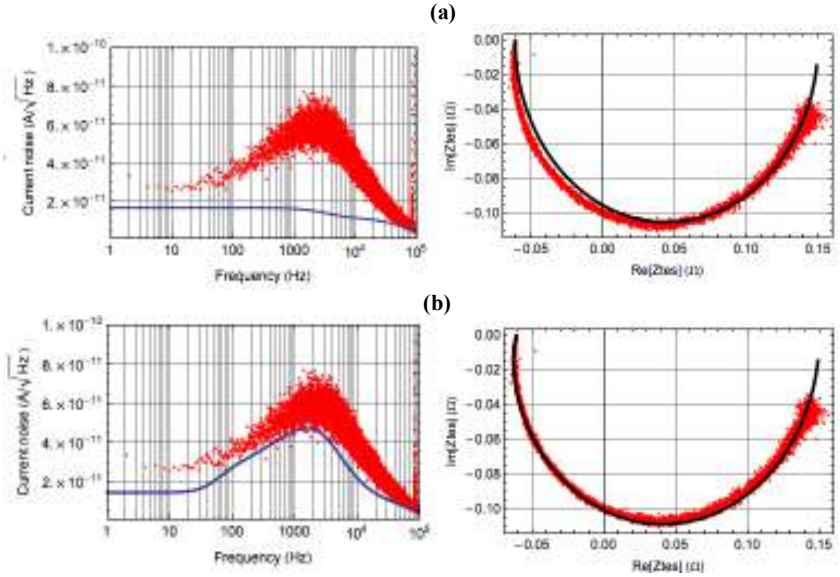

Fig. 2. Measured (red dots) noise and complex impedance compared with calculated (solid lines) values using (a) simple TES model (n = 0) and (b) distributed leg model (n =10). The bias point is 30% in the transition.

3. LOW NOISE DESIGN GUIDLINE

The measured NEP of the TES in Fig. 2 is 2×10^{-18} W/√Hz, which is about an order of magnitude higher than what is required for the SAFARI. In order to reduce the NEP we need to lower the G. Assuming that G scales with the leg geometry this can be realized by combination of increasing the length, decreasing the width and reducing the membrane thickness.

A Distributed TES Model for Designing Low Noise Bolometers

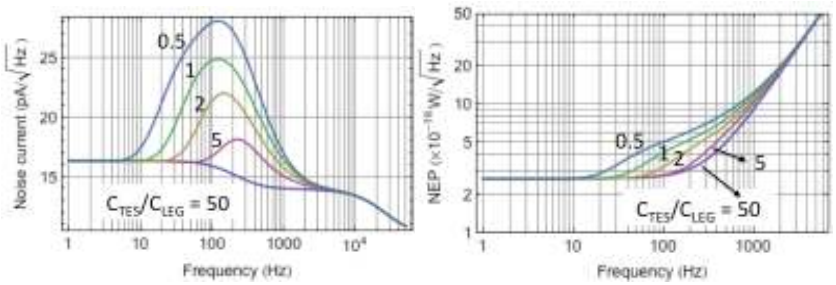

Fig. 3. Calculated noise and NEP using the distributed model (n =10) for different heat capacity in the legs. In all cases the heat capacity of TES (C_{TES}) is 5 fJ/K and total heat conductance is 0.3 pW/K. The bias point is the same and at 30% in the transition.

In principle we can achieve a certain G using different leg geometries and the distributed leg model enables us to calculate the noise for different designs. Fig. 3 shows the calculated noise current spectra and the corresponding NEP for TES with the same G but different leg mass. A Tc of 100 mK is used which gives an NEP of about 3×10^{-19} W/√Hz. Here the C_{TES} is set to 5 fJ/K but the total heat capacity of the legs (C_{LEG}) varies between 0.5 to 50 times smaller than C_{TES}.

It is clear that the lighter the legs, the lower the excess noise bump. The lower the total G, the slower the device and therefore the noise role-off frequency is lower. In case of very low-G devices with heavy legs, the low frequency tail of the noise bump can be stretched well below 10 Hz, where it merges with 1/f noise. As a result the measured dark NEP would be larger.

To confirm this hypothesis we compare two devices one with heavy legs (TES #1) and the other one with light legs (TES #2). Table 1 summarized some of the important parameters of these devices.

Table 1 Parameters of the devices

Parameter	TES #1	TES #2
Leg length [μm]	1310	400
Leg width [μm]	6.5	1
Mem. thick. [μm]	1	0.5
TES size [μm^2]	110×110	50×50
Mem. size [μm^2]	140×140	160×160
T_c [mK]	75	78
R_N [mΩ]	212	103
Sat. power [fW]	9	10
G [pW/K]	0.38	0.33
NEP [W/√Hz]	6.5×10^{-19}	4.2×10^{-19}

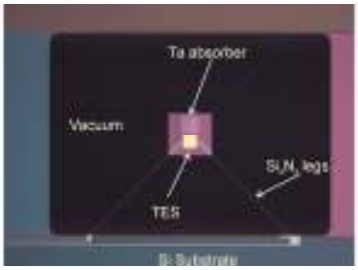

Fig. 4 TES #2 fabricated on 0.5 μm thick 160×160 μm^2 SiN island supported by 1 μm wide and 400 μm long SiN legs.

As we see in Table 1, the T_c, saturation power and the G of these two are very similar but note that the legs of the TES #1 are about 42 times heavier than TES #2. Although the membranes and the TES sizes are not the same, we believe that the main difference between the two devices is the mass of the legs. Fig. 5 shows the noise current spectra at different bias points. It is evident that the excess noise bumps seen in TES #1 are not present in TES #2 as expected from the model. We measured lower dark NEP of 4.2×10^{-19} W/√Hz for the latter. The conclusion is that in order to achieve low NEP it is essential to fabricate low-G TES devices with as light as possible supporting legs. This means that they should be made as narrow as possible on as thin as possible membrane and only as long as necessary.

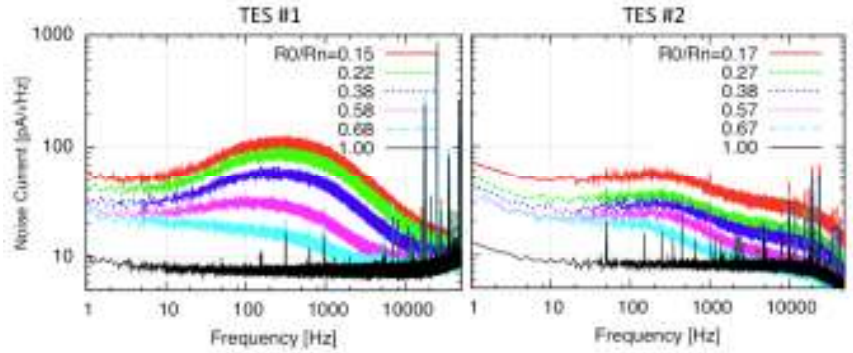

Fig. 5 Noise current spectra of heavy legs (TES #1) and light legs (TES #2) devices. TES #1 has 42 times heavier legs than the TES #2.

REFERENCES

[1] H. Kaneda, T. Nakagawa, T. Onaka, T. Matsumoto, H. Murakami, K. Enya, H. Kataza, H. Matsuhara, and Y. Y. Yui, In Proc. SPIE Optical, Infrared, and Millimeter Space Telescopes, vol. 5487, p. 991 (2004)

[2] B. Swinyard, In Proc. SPIE Space Telescopes and Instrumentation I: Optical, Infrared, and Millimeter, vol. 6265, no. 1, p. 62650L (2006)

[3] M. A. Lindeman, S. Bandler, R. P. Brekosky, J. A. Chervenak, E. Figueroa-Feliciano, F. M. Finkbeiner, M. J. Li, and C. A. Kilbourne, Rev. Sci. Instrum., vol. 75, p. 1283 (2004)

[4] K.D. Irwin and G.C. Hilton, Cryogenic Particle Detection, Transition-Edge Sensors, Topics in Applied Physics, vol. 99, p. 92 (2005)

[5] M. A. Lindeman, Ph. D. Thesis, (2000), Available online at: http://www.osti.gov/energycitations/product.biblio.jsp?osti_id=15009469

[6] P. Khosropanah, B. P. F. Dirks, M. Parra-Borderías, M. Ridder, R. Hijmering, J. van der Kuur, L. Gottardi, M. Bruijn, M. Popescu, J. R. Gao, and H. Hoevers, IEEE Trans. Appl. Superconductivity, vol. 21, No. 3, P. 236 (2011)